Modified TNO-Blake model for aerofoil surface pressure prediction with canopies

Suresh Palani*, Chaitanya Paruchuri †, Phillip Joseph‡
Institute of Sound and Vibration Research, University of Southampton, Southampton, SO17 1BJ, UK

Sergey Karabasov§, Annabel Markesteijn ¶
School of Engineering and Materials Science, Queen Mary University of London, London, E1 4NS, UK

Tze Pei Chong‖
Department of Mechanical and Aerospace Engineering, Brunel University London, London, Uxbridge UB8 3PH, UK

Abstract

The modelling of the surface pressure spectrum beneath a turbulent boundary layer near the trailing edge of an aerofoil with bio-inspired surface treatments, called canopies, is investigated. Canopies are simply a cylindrical rods uniformly spaced along the span of the aerofoil. The velocity measurements indicated that the flow at the trailing edge of an aerofoil treated with canopies is localised and shows periodic behaviour across the span with treatment spacing. As a result, the mean-flow velocity gradient along the span ($\partial U_1/\partial x_3$) cannot be assumed as zero for x_2/h = 4, which is shown in this paper. Therefore, the original surface pressure solution of Poisson's equation is modified by introducing an additional source term consisting of the mean-shear contribution, given as $\partial U_1/\partial x_3\ \partial u_3/\partial x_1$. Furthermore, the surface pressure attenuation due to the canopies shows a periodic behaviour across the span for treatments with an Open-Area-Ratio (OAR) between 70% and 90 %. This observation is consistent with our previous experimental results; therefore, the primary motivation for proposing a 3D TNO-Blake model, accounting for the interaction between the gradient of the stream-wise mean velocity along the span and span-wise fluctuating component along the stream. The model is built based on the inputs from Large Eddy Simulation results and additional wind tunnel measurements.

I. Introduction

Aerofoil trailing edge noise is generated when the pressure fluctuations, caused by the boundary layer turbulence in the vicinity of the aerofoil surface, convect downstream past the trailing edge. Therefore, reducing the unsteady surface pressure fluctuations at the trailing edge can lead to significant aerofoil self-noise reductions, especially for surfaces interacting with airflow, like wind turbines and turbofans. With the rapid increase in wind-energy expansion, more effective designs of surface treatments are required to attain the desired levels of noise reduction to meet future clean energy requirements.

In this paper, we attempt to develop a semi-analytical prediction technique of the surface pressure spectrum beneath a turbulent boundary layer near the trailing edge of the aerofoil in the presence of bio-inspired surface treatments called canopies, using the TNO-Blake model. This study is motivated by the experimental works at the Virginia Tech Anechoic wall-jet facility, beginning with Clark et al. [1] study on bio-inspired surface treatments, called canopies, based on the structure of the owl's downy coating. The experiments showed that the canopies placed at the height of

*Senior Research Assistant, Institute of Sound and Vibration Research (ISVR), S.Palani@soton.ac.uk.
†RAEng Research Fellow and lecturer, Institute of Sound and Vibration Research (ISVR), ccp1m17@soton.ac.uk.
‡Professor, Institute of Sound and Vibration Research (ISVR), pfj@soton.ac.uk.
§Professor of Computational Modelling, Queen Mary University of London, s.karabasov@qmul.ac.uk.
¶Postdoctoral Research Assistant, Queen Mary University of London, a.markesteijn@qmul.ac.uk.
‖Lecturer, Brunel University London, t.p.chong@brunel.ac.uk.

nearly 40% of the boundary layer thickness from the wall with fibres oriented in the flow direction provided surface pressure attenuation up to 30 dB at higher frequencies. Furthermore, they found that attenuation increased exponentially with frequency and depended on the flow velocity. Later, Clark et al. [2] designed surface treatments called finlet fences and rails by modifying the unidirectional canopies, which were mounted on a DU96-W180 airfoil trailing edge. This experimental work showed a far-field noise reduction of up to 10 dB between 2 and 5 kHz with surface treatments using beamforming. Most other surface treatment works mainly focused on finlet fences to reduce trailing edge noise [3–5]. Bodling and Sharma [6] numerically investigated the Finlet fences proposed by Clark et al. [2] on NACA0012 aerofoil. The authors observed that the normalised turbulence kinetic energy is redistributed from the trailing edge surfaces of the aerofoils to the Finlet fences. The surface treatments were effective over a range of angle-of-attack that extends to over 9 deg from zero-lift. In addition, aerofoil treatments did not adversely affect aerodynamic performances. Also, the experimental work of Clark et al. [2] included a brief study on the Finlet rail, a series of rods supported from the aerofoil trailing edge surface. This work focused on the effect of Finlet rail extension, height, and doubling of the diameter and spacing on the radiated trailing edge noise spectra. Clark et al. [2] showed that increasing the height of the Finlet rails from the aerofoil trailing edge surface deteriorates the noise reduction benefits. This observation was associated with the prevention of the smaller-scale turbulent fluctuations from being de-correlated along the aerofoil span. Additionally, the work of Clark et al. [2] showed a decrease in noise reduction due to increased rails (canopies) height. These findings from previous studies, directly conducted on the aerofoil, where the fences or canopies-like surface treatments were hypothesised to be lifting low-frequency flow structures from the trailing edge, are inconclusive.

Gonzalez et al. [7] focused on more fundamental studies on understanding pressure shielding mechanisms from canopies like surface treatments. These canopy structures are unidirectional rod treatments. Gonzalez et al. [7] performed experimental and computational analysis on canopy surface treatments which showed a reduction in the surface pressure fluctuations. Gonzalez et al. [7] also developed a prediction method for the surface pressure spectrum through a combination of the RANS solution data and a theoretical surface pressure model. The pressure fluctuations on the surface are then solved by modelling the linear term in Poisson's equation and integrating them along the wall-normal direction. However, the prediction model developed by Gonzalez et al. [7]and Hari et al. [8] did not include the periodic distribution of the velocity in the vicinity of surface treatments.

The wall pressure fluctuations in the turbulent boundary layer can be obtained by solving the Poisson equation, which is derived by taking the divergence of the incompressible momentum equation and then subtracting the time-averaged quantities from the fluctuating ones, and is given as

$$\nabla^2 p = -2\rho \frac{\partial^2 U_i u_j}{\partial x_i \partial x_j} - \rho \frac{\partial^2}{\partial x_i \partial x_j} \left(u_i u_j - \overline{u_j u_j} \right) \tag{1}$$

where ∇^2 is the Laplacian operator, ρ is the fluid density, U_i and u_i are the mean and fluctuating velocity for the i-th component in the i-th direction, respectively. The first term on the right side of Eqn. 1 represents the interactions between the mean-shear and the turbulence, while the second term represents turbulence-turbulence interactions. In shear flows, the mean-shear and turbulence interactions are an order of magnitude higher than the turbulence-turbulence interactions [9]. Therefore, the second term (turbulence-turbulence interactions) are ignored.

Figure 1 shows the contour plot of the mean distribution of stream-wise velocity (U_1) downstream of the trailing edge at $x/c = 1.01$, for a representative canopy case of $d = 1$ mm and $s = 4$ mm with an Open-Area-Ratio of 75 %. The height h of the canopy from the aerofoil surface is 6 mm. The x_3 (span) and x_2 (normal to the aerofoil surface) distances covered are normalised by the canopy spacing (s) and height (h), respectively. Therefore, the canopies are located at 0, 1, and 2. The hot-wire measurements were made for the velocity of 40 m/s.

The figure also clearly shows that the velocity distribution at the aerofoil trailing, treated with canopies, at $x_2/h = 1$ is periodic in x_3 (across the span), whose period is equal to s. Therefore, we assume that the span-wise variation in the stream-wise mean velocity (U_1), at a single frequency, can be simply given by

$$U_1 \left(x_2, x_3\right) = \sum_{n=-\infty}^{\infty} U_{1,n} \left(x_2\right) e^{-j k_{3,n} x_3} \tag{2}$$

where $k_{3,n} = n\pi/s$ and the stream-wise mean velocity is given by $U_{1,0}\left(x_2\right)$. Similarly, the fluctuating component is given by,

$$u_i \left(x_1, x_2, x_3\right) = \sum_{m=-\infty}^{\infty} u_{3,m} \left(x_2\right) e^{-j\left(K_1 x_1 + K_{3,m} x_3\right)} \tag{3}$$

where $k_1 = \omega/U_c\ (x_2, x_3)$ and $i = 2$, and 3.

The point $x_3/s = 0$ here coincides with the centre of the canopy rod as shown by the shaded region.

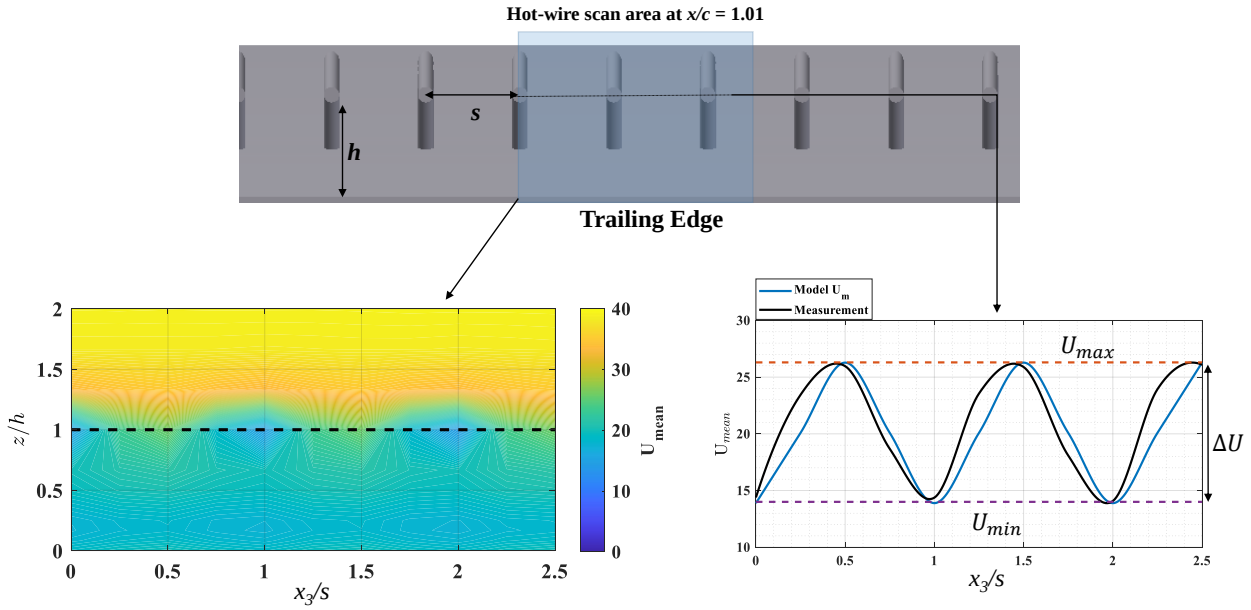

Fig. 1 Picture of the test section and schematic of a NACA0012 aerofoil trailing edge with canopies.

From Fig. 1, it is clear that the mean-flow velocity gradient term, in Eqn. 1, along the span ($\partial U_1/\partial x_3$) cannot be assumed as zero. Therefore, the original TNO-Blake model is modified here by introducing an additional source term consisting of the mean-shear contribution, given as $\frac{\partial U_1}{\partial x_3}\frac{\partial u_3}{\partial x_1}$, in the linear source term of Poisson's equation ([10, 11]) and is given by

$$\nabla^2 p\,(\mathbf{x},t) = -2\rho\left(\frac{\partial U_1}{\partial x_2}\frac{\partial u_2}{\partial x_1} + \frac{\partial U_1}{\partial x_3}\frac{\partial u_3}{\partial x_1}\right) = q\,(\mathbf{x},t)\,. \tag{4}$$

where $\partial U_1/\partial x_2$ and $\partial U_1/\partial x_3$ denotes the mean velocity gradient, u_2 and u_3 are the wall-normal, and span-wise turbulent velocity component, respectively. In Eqn. 4, the mean velocity gradient ($\partial U_1/\partial x_2$ and $\partial U_1/\partial x_3$) is obtained from the LES calculations performed using the in-house code developed by Sergey and Annabel.

As a result, the aim of the preliminary work described in this paper is to develop a semi-analytical prediction technique of the surface pressure spectrum beneath a turbulent boundary layer near the trailing edge of the aerofoil in the presence of bio-inspired surface treatments called canopies by extending the TNO-Blake model.

II. Experimental set-up

The aerofoil noise measurements were carried out at the ISVR's open-jet wind tunnel facility. The wind tunnel nozzle is mounted inside an anechoic chamber of dimensions 8 m x 8 m x 8 m, and the size of the nozzle exit is 150 mm x 450 mm with a contraction ratio of 25:1. It provides a quiet and low-turbulence flow (<0.4 %) for aerofoil noise measurements. The maximum flow speed at the exit of the nozzle is 100 m/s. However, the aerofoil noise measurements were made at speeds 20, 40, and 60 m/s. As shown in **Fig. 2**, far-field noise measurements were made using 15 half-inch condenser microphones (B&K type 4189) located in the mid-span plane of the aerofoil and at a constant radial distance of 1.2 m from the aerofoil mid-chord position. In this study, the 0.2 m chord NACA0012 aerofoil was used for the experiments. As shown in Fig. **??**, the experimental test section consists of NACA0012 aerofoil supported by side plates. The side plates were flush mounted at the nozzle exit section and maintains the flow two-dimensionality. The aerofoil noise was measured at 0, 5^o and 10^o angle of attack (α). The aerofoils with surface treatments were 3-D printed in two parts for the ease of manufacturing and testing using a Stereolithography (SLA) printer. **Fig. 3** shows the second part of the aerofoil, of length 90 mm, with surface treatments starting from x/c =0.575. The incoming flow was tripped on

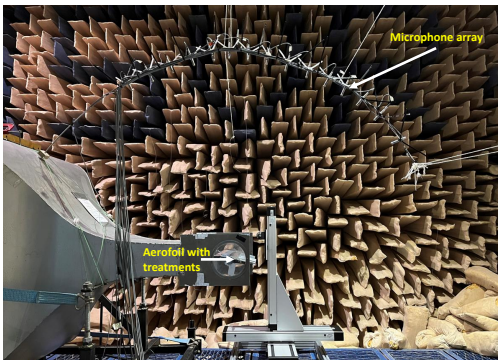

Fig. 2 Test set-up for aerofoil noise measurement. Shown in the picture are the open-jet wind tunnel nozzle, NACA0012 aerofoil, microphone polar array, and hot-wire traverse system.

both suction and pressure sides to prevent tonal noise generation due to Tollmien-Schlichting waves convecting in the laminar boundary layer the flow. For tripping the flow, a rough band of tape of width 2.5 cm was applied at 10% of chord from the leading edge. The tape has roughness of SS 100, corresponding to a surface roughness of 140 μm.

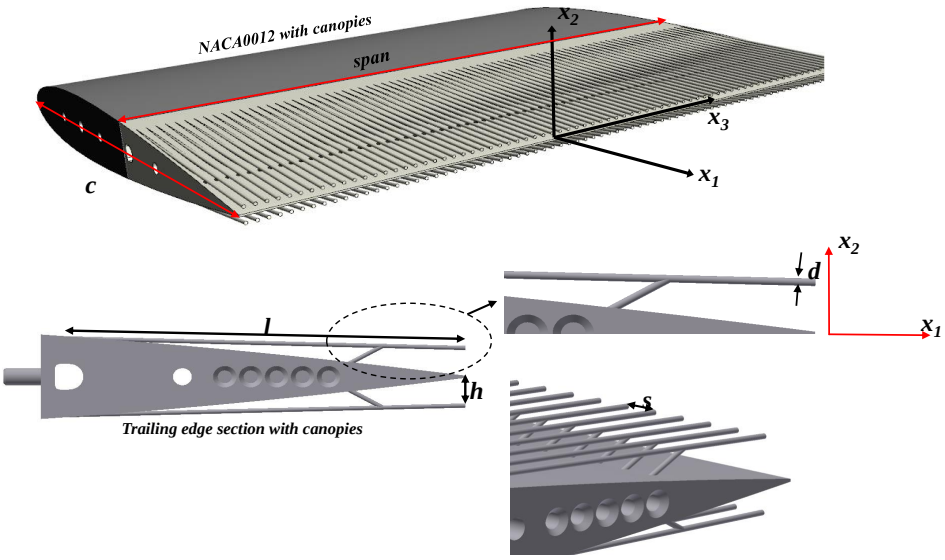

Fig. 3 CAD geometry of the NACA0012 aerofoil with surface treatments.

For the far-field noise measurements, the microphones are placed at radiation angles(θ) of between 30^o and 120^o measured relative to the aerofoil mid-chord position. The noise measurements were made for a time duration of 10 sec at a sampling frequency of 40 kHz. In the post processing, the noise spectra was calculated with a window size of 512 data points corresponding to a frequency resolution of 78.125 Hz.

Fig. 3 shows the schematic of the NACA0012 trailing edge treated with canopy. For this experiment, we set the non-dimensional height for the canopy (h/δ), spacing between the canopy ($(s-d)/s$), and length (l/h) to vary between 0.08 and 0.5, 0.2 and 0.9, and 0 and 53.3, respectively.

III. Surface Pressure Attenuation: Span-wise variation

The unsteady surface pressure was measured at five locations on NACA0012 aerofoil using the miniature microphones, Knowles FG-23329-P07 type, along the span and chord around $x/c = 0.98$. The pressure sensors are attached to the

aerofoil surface remotely. The pressure sensors' locations are chosen to cover the x_3/s between 0.5 and 1.5. As shown in the **Fig. 4**, Mic-7 and Mic-8 are directly located below the canopy at traverse location $x_3/s = 1$.

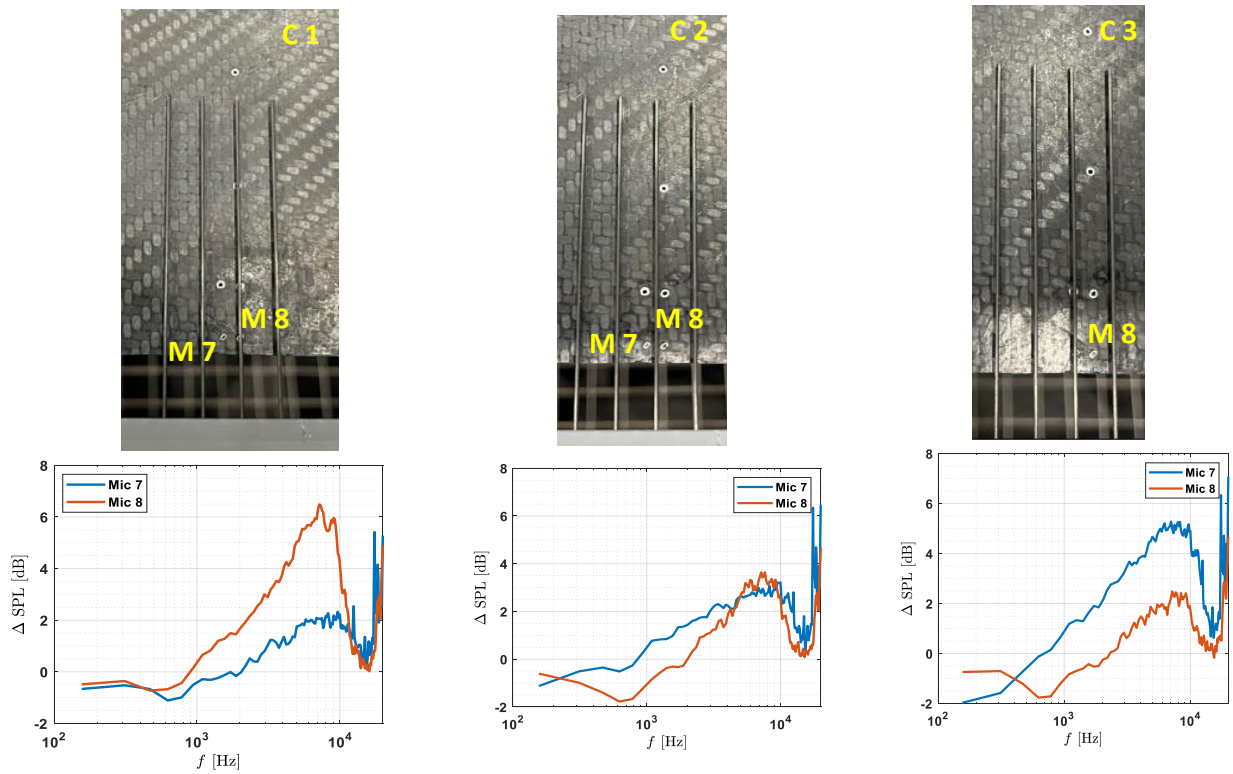

Fig. 4 Picture of the test section and the surface pressure measurement on NACA0012 aerofoil trailing edge with canopies.

Fig. 4 shows the attenuation in the unsteady surface pressure spectra due to the canopies at mean-flow speed U_∞ = 20 m/s. Significant reduction in the surface pressure is noticeable only from the sensor, which is directly located below the canopies. For example, from **Fig. 4** (a), it can be seen that the surface pressure reduction level tends to increase steadily for mic 8 located at x_3/s =1, reaching a maximum of 8 dB. However, the reductions from the mic 7 located at x_3/s =0.5, away from the canopies are not that significant. This observation is consistent for all the mean-flow velocities and the results are not included here for brevity.

IV. Surface Pressure Modelling: A Modified TNO-Blake Model

As stated earlier, in this paper we attempt to develop a model to predict the surface pressure spectrum beneath a turbulent boundary layer near the trailing edge of the aerofoil in the presence of bio-inspired surface treatments, called canopies, using the TNO-Blake model. The modified TNO-Blake model is an extension based on the formulations originally proposed by of Kraichnan [9] and Blake [10] for predicting the single point wall pressure spectrum on the surface of a flat plate subjected to external flow.

A. Modified TNO-Blake Model

In this section, the important part of the revised TNO-Blake model for predicting the single point spectra based on the location along the span, where the mean and fluctuating velocity profiles are estimated, is derived. The assumptions made to obtain a solution to the governing Eqn. 4 are as follows:

1) assuming some degree of periodicity in the mean velocity along the span, which is given by Eqn. 3

2) the integral length scale λ characterizes the size of the energy-containing eddies and is a local quantity depending on the distance from the wall is estimated using the stream-wise velocity spectrum as shown in Fig. **??**.
3) the turbulent flows in the boundary layer in the presence of canopies are not perfectly homogeneous and isotropic. Still, the turbulence spectral tensor components derived using the von Karman isotropic theory were used in this preliminary prediction.

Please note this is only a first attempt to model and predict the surface pressure by accounting for the presence of span-wise periodic structures, canopies, in a turbulent boundary layer. In future, we aim to improve this proposed model by reducing the assumptions using the LES data.

The Eqn. 4 is solved by Fourier transforming the equation to the frequency-wavenumber space. For a turbulent boundary layer flows over a flat plate without canopies, it is reasonable to assume that the flow is homogeneous in the streamwise, x_1 and spanwise x_3 directions. However, for the canopy cases as shown here, the flow is no more homogeneous along the span. Therefore, the inverse Fourier transform for $q(\mathbf{x},t)$ can be written as,

$$q(\mathbf{x},t) = \int\int\int_{-\infty}^{\infty} \tilde{q}(k_1,x_2,k_3,\omega)\, e^{-i\omega t + ik_1x_1 + ik_3x_3}\, d\omega dk_1 dk_3 \tag{5}$$

Similarly, the resultant pressure field can also be represented as,

$$p(\mathbf{x},t) = \int\int\int_{-\infty}^{\infty} \tilde{p}(k_1,x_2,k_3,\omega)\, e^{-i\omega t + ik_1x_1 + ik_3x_3}\, d\omega dk_1 dk_3 \tag{6}$$

where $k_1 = \omega/U_c\,(x_2,x_3)$ and $i = 2$, and 3. U_c is assumed to be $0.5U_\infty$ for the canopy cases, based on the stream-wise surface pressure phase measurements.

By replacing the terms in the governing Eqn. 4 with their spectral forms as given in Eqns. 5 and 6 and equating the integrands can give the Poisson's equation in the frequency-wavenumber domain as

$$\frac{\partial^2 \tilde{p}(k_1,x_2,k_3,\omega)}{\partial x_2^2} - \left[k_1^2 + k_3^2\right]\tilde{p}(k_1,x_2,k_3,\omega) = \tilde{q}(k_1,x_2,k_3,\omega)\,. \tag{7}$$

The inhomogeneous linear second-order equation given by Eqn. 7 can by solved by using the method of variations of parameters, following the steps similar to the one described in Ref. [12] a solution for the wavenumber-frequency surface pressure spectrum can be obtained as an integral across the boundary layer

$$\tilde{p}(k_1,x_2=0,k_3,\omega) = \frac{1}{k}\int_0^{\delta_{BL}} e^{-ky_2}\tilde{q}(k_1,y_2,k_3,\omega)\, dy_2 \tag{8}$$

where $\tilde{q}(k_1,y_2,k_3,\omega)$ is the wavenumber-frequency form of the source term and is given as,

$$\begin{aligned}\tilde{q}(k_1,y_2,y_3,\omega) = \sum_{n=-\infty}^{\infty}\tilde{q}(k_1,y_2,k_{3n},\omega) = -2\rho_o \underbrace{\left(\sum_{n=-\infty}^{\infty}\frac{\partial U_{1,n}(y_2)}{\partial y_2}e^{-jk_{3,n}y_3}\right)\left(\sum_{m=-\infty}^{\infty}-jk_1\tilde{u}_{2,m}e^{-j\left(k_1y_1+k_{3,m}y_3\right)}\right)}_{(\partial U_1/\partial x_2)(\partial u_2/\partial x_1)} \\ - 2\rho_o \underbrace{\left(-jk_{3,n}\sum_{n=-\infty}^{\infty}U_{1,n}(y_2)\,e^{-jk_{3,n}y_3}\right)\left(-jk_1\sum_{m=-\infty}^{\infty}\tilde{u}_{3,m}e^{-j\left(k_1y_1+k_{3,m}y_3\right)}\right)}_{(\partial U_1/\partial x_3)(\partial u_3/\partial x_1)}.\end{aligned} \tag{9}$$

$$\begin{aligned}\tilde{q}(k_1,y_2,y_3,\omega) = -2\rho_o \underbrace{\left(\sum_{n=-\infty}^{\infty}\frac{\partial U_{1,n}(y_2)}{\partial y_2}e^{-jk_{3,n}y_3}\right)\left(\sum_{m=-\infty}^{\infty}-jk_1\tilde{u}_{2,m}e^{-j\left(k_1y_1+k_{3,m}y_3\right)}\right)}_{(\partial U_1/\partial x_2)(\partial u_2/\partial x_1)} \\ - 2\rho_o \underbrace{\left(-jk_{3,n}\sum_{n=-\infty}^{\infty}U_{1,n}(y_2)\,e^{-jk_{3,n}y_3}\right)\left(-jk_1\sum_{m=-\infty}^{\infty}\tilde{u}_{3,m}e^{-j\left(k_1y_1+k_{3,m}y_3\right)}\right)}_{(\partial U_1/\partial x_3)(\partial u_3/\partial x_1)}.\end{aligned} \tag{10}$$

Finally, the wavenumber-frequency spectra of the wall-pressure is given by the ensemble average of the product of $\tilde{p}\left(k_1, x_2 = 0, k_3, \omega\right)$ (Eqn. 8) with its complex conjugate

$$E\left[\tilde{p}\left(k_1, x_2 = 0, y_3, \omega\right)\tilde{p}^*\left(k_1, x_2 = 0, y_3, \omega\right)\right] = S_{pp}(k_1, y_3, \omega)\delta\left(\omega - \omega'\right)\delta\left(k_1 - k_1'\right)\delta\left(k_3 - k_3'\right) \tag{11}$$

Now by substituting the solution given in Eqns. 8 and 9 into the previous equation, assuming $m = m'$ in the fluctuating components, and integrating over the whole primed frequency and wavenumber space yields

$$\begin{aligned} S_{pp}(k_1, y_3, \omega) = \sum_{n=-\infty}^{\infty} S_{pp}(k_1, k_{3n}, \omega) = \frac{4\rho_o^2 k_1^2}{k^2}\int_0^{\delta_{BL}}\int_0^{\delta_{BL}}\Bigg[\sum_{n=-\infty}^{\infty}\sum_{n'=-\infty}^{\infty}\left(\frac{\partial U_{1,n}}{\partial y_2}\frac{\partial U_{1,n'}}{\partial y_2'}e^{-jy_3\left(k_{3,n}-k_{3,n'}\right)}\right)\sum_{m=-\infty}^{\infty}E\left[\tilde{u}_{2,m}\tilde{u}_{2,m}^*\right]\Bigg] \\ + j\Bigg[\sum_{n=-\infty}^{\infty}\sum_{n'=-\infty}^{\infty}\left(k_{3,n'}\frac{\partial U_{1,n}}{\partial y_2}U_{1,n'}e^{-jy_3\left(k_{3,n}-k_{3,n'}\right)}\right)\sum_{m=-\infty}^{\infty}E\left[\tilde{u}_{2,m}\tilde{u}_{3,m}^*\right]\Bigg] \\ - j\Bigg[\sum_{n=-\infty}^{\infty}\sum_{n'=-\infty}^{\infty}\left(k_{3,n}U_{1,n}\frac{\partial U_{1,n'}}{\partial y_2'}e^{-jy_3\left(k_{3,n}-k_{3,n'}\right)}\right)\sum_{m=-\infty}^{\infty}E\left[\tilde{u}_{3,m}\tilde{u}_{2,m}^*\right]\Bigg] \\ + \Bigg[\sum_{n=-\infty}^{\infty}\sum_{n'=-\infty}^{\infty}\left(k_{3,n}k_{3,n'}U_{1,n}U_{1,n'}e^{-jy_3\left(k_{3,n}-k_{3,n'}\right)}\right)\sum_{m=-\infty}^{\infty}E\left[\tilde{u}_{3,m}\tilde{u}_{3,m}^*\right]\Bigg] \\ e^{-2k\left(y_2+y_2'\right)}dy_2dy_2' \end{aligned} \tag{12}$$

where the ensemble averaging of the velocity fluctuation terms $E\left[\tilde{u}_{i,m}\left(k_1, k_{3m}, y_2, y_2', \omega\right)\tilde{u}_{j,m}^*\left(k_1, k_{3m}, y_2, y_2', \omega\right)\right]$ in the above equations can be expressed as, based on the assumptions made by Blake [13],

$$\begin{aligned} E\left[\tilde{u}_{i,m}\left(k_1, k_{3m}, y_2, \omega\right)\tilde{u}_{j,m}^*\left(k_1, k_{3m}, y_2', \omega\right)\right] = L_{ij}(y_2)\delta\left(y_2 - y_2'\right) \\ \sqrt{\overline{u^2}_{im}(y_2)\overline{u^2}_{jm}(y_2')}\phi_{ijm}\left(k_1, k_{3m}, y_2, \omega\right)\Delta\left(\omega - U_c(y_2)k_1\right) \end{aligned} \tag{13}$$

In Eqn. 13, $L_{ij}(y_2)$ is the correlation length, $\phi_{ijm}\left(k_1, k_{3m}, y_2, \omega\right)$ is the turbulence spectral tensor components derived using the von Karman isotropic theory ,and $\sqrt{\overline{u^2}_{im}\overline{u^2}_{jm}}$ is the mean square velocity components.

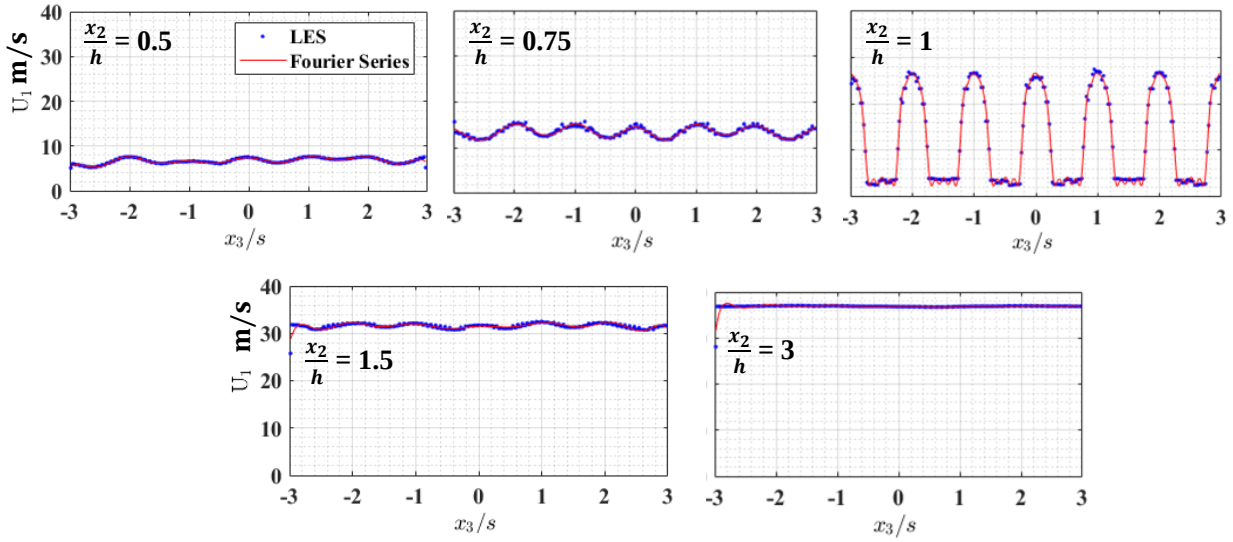

(a) d = 1 mm, s =2 mm, h = 2 mm

Fig. 5 Mean velocity distribution along the span for Canopies with diameter 1 and 2 mm at height = 2 mm. Mean-flow velocity is 40 m/s. LES data captured at x_1/c = 0.96

Fig. 5 shows the mean velocity distribution at $x_1/c = 0.96$. The x_3 (span-wise) distance is normalised by the canopy spacing (s). The canopies are located at -2.5,-1.5,-0.5, 0.5, 1.5, and 2.5. As mentioned earlier, the LES simulations were made for the free stream (U_∞) velocity of 40 m/s. Comparing the mean velocity distribution along the span at different heights inside the boundary layer shows the influence of the surface treatments on the flow structure. As mentioned earlier, the significant effect on the flow is noticeable only close to the canopy heights ($x_2/h = 1$). Also, these results indicate that the mean flow gradient along the span responsible for the additional source term in the Poisson's equation decreases gradually as we move away from the canopies.

In **Fig. 5**, the Fourier summation representing the mean-flow span-wise variation is also included, given by Eqn. 2, which showed good convergence with the LES results for 7 terms summation.

Fig. 6 shows the profiles of mean-square velocity components ($\overline{u^2}_1$,$\overline{u^2}_2$, and $\overline{u^2}_3$) at the NACA0012 aerofoil trailing edge treated with canopies. It is observed that there exists a consistently periodic behaviour in the mean-squared velocity components in the LES data for the NACA0012 aerofoil treated with canopies. This may suggest the assumption of mean and fluctuating velocity components using Fourier series summation in the model to accurately capture the surface pressure in the turbulent boundary layer for aerofoils treated with canopy-like surface treatments. Additionally, from these figures, it can be concluded that the stretching factors, in particular β_2 and β_3, cannot be assumed to be constants.

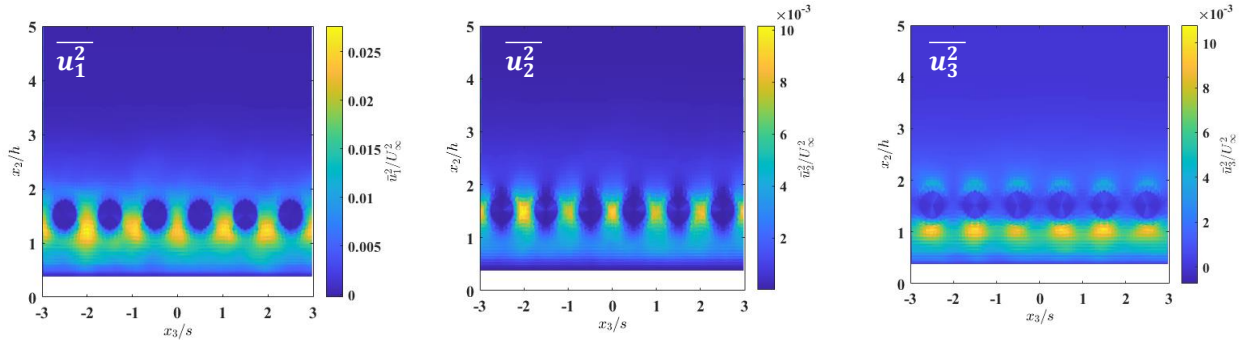

Fig. 6 The profiles of mean-square velocities ($\overline{u^2}_1$,$\overline{u^2}_2$, and $\overline{u^2}_3$) at the NACA0012 aerofoil trailing edge treated with canopies.

V. Summary and Future plan

In this paper, the modelling of the surface pressure spectrum beneath a turbulent boundary layer near the trailing edge of an aerofoil with bio-inspired surface treatments, called canopies, is investigated using the LES data. The mean velocity and mean-squared velocity components indicated that the flow at the trailing edge of an aerofoil treated with canopies is localised and shows periodic behaviour across the span with treatment spacing. Consequently, the mean-flow velocity gradient along the span ($\partial U_1/\partial x_3$) cannot be assumed as zero, as shown in this paper. Therefore, the original surface pressure solution of Poisson's equation is modified by introducing an additional source term consisting of the mean-shear contribution, given as $\partial U_1/\partial x_3 \; \partial u_3/\partial x_1$. Furthermore, the surface pressure attenuation due to the canopies shows a periodic behaviour across the span for treatments for selected Open-Area-Ratio ((OAR) between 70% and 90 %).

In the future, we plan to conduct a detailed analysis using the LES data to improve the accuracy of the 3-D TNO/Blake model for predicting the surface pressure in the vicinity of surface treatments. Additionally, the contribution of each term to the surface pressure Eqn. 12 will be investigated in detail.

Acknowledgments

This project has received funding from the EPSRC under grant No EP/V038273/1.

References

[1] Clark, I. A., Daly, C. A., Devenport, W., Alexander, W. N., Peake, N., Jaworski, J. W., and Glegg, S., "Bio-inspired canopies for the reduction of roughness noise," *Journal of Sound and Vibration*, Vol. 385, 2016, pp. 33–54. https://doi.org/https://doi.org/10.1016/j.jsv.2016.08.027.

[2] Clark, I. A., Alexander, W. N., Devenport, W., Glegg, S., Jaworski, J. W., Daly, C., and Peake, N., "Bioinspired Trailing-Edge Noise Control," *AIAA Journal*, Vol. 55, No. 3, 2017, pp. 740–754. https://doi.org/10.2514/1.J055243.

[3] Afshari, A., Azarpeyvand, M., Dehghan, A. A., and Szőke, M., "Effects of Streamwise Surface Treatments on Trailing Edge Noise Reduction," 2017, pp. 1–17. https://doi.org/10.2514/6.2017-3499.

[4] Afshari, A., Azarpeyvand, M., Dehghan, A. A., Szőke, M., and Maryami, R., "Trailing-edge flow manipulation using streamwise finlets," *Journal of Fluid Mechanics*, Vol. 870, 2019, p. 617–650. https://doi.org/10.1017/jfm.2019.249.

[5] Gstrein, F., Zang, N., and Azarpeyvand, M., "Application of Finlets for Trailing Edge Noise Reduction of a NACA 0012 Airfoil," *AIAA AVIATION 2020 FORUM*, 2020, pp. 1–16. https://doi.org/10.2514/6.2020-2502.

[6] Bodling, A., and Sharma, A., "Numerical investigation of noise reduction mechanisms in a bio-inspired airfoil," *Journal of Sound and Vibration*, Vol. 453, 2019, pp. 314–327. https://doi.org/https://doi.org/10.1016/j.jsv.2019.02.004.

[7] Gonzalez, A., Glegg, S. A., Hari, N., and Devenport, W. J., "Fundamental Studies of the Mechanisms of Pressure Shielding," *25th AIAA/CEAS Aeroacoustics Conference*, 2019, pp. 1–25. https://doi.org/10.2514/6.2019-2403.

[8] Hari, N. N., Szoke, M., Devenport, W. J., Glegg, S. A., Priddin, M. J., and Ayton, L. J., "Experimental investigation of Bio-inspired Unidirectional Canopies," *AIAA AVIATION 2021 FORUM*, ????, pp. 1–16. https://doi.org/10.2514/6.2021-2262.

[9] Kraichnan, R. H., "Pressure fluctuations in turbulent flow over a flat plate," *Journal of the Acoustical Society of America*, Vol. 28, No. 3, 1956, pp. 378–390. https://doi.org/10.1121/1.1908336.

[10] Blake, W. K., "Turbulent boundary-layer wall-pressure fluctuations on smooth and rough walls," *Journal of Fluid Mechanics*, Vol. 44, No. 4, 1970, p. 637–660. https://doi.org/10.1017/S0022112070002069.

[11] Blake, W. K., "Chapter 2 - Essentials of Turbulent Wall Pressure Fluctuations," *Mechanics of Flow-Induced Sound and Vibration, Volume 2 (Second Edition)*, edited by W. K. Blake, Academic Press, 2017, second edition ed., pp. 81–177. https://doi.org/https://doi.org/10.1016/B978-0-12-809274-3.00002-7, URL https://www.sciencedirect.com/science/article/pii/B9780128092743000027.

[12] Grasso, G., Jaiswal, P., Wu, H., Moreau, S., and Roger, M., "Analytical models of the wall-pressure spectrum under a turbulent boundary layer with adverse pressure gradient," *Journal of Fluid Mechanics*, Vol. 877, 2019, p. 1007–1062. https://doi.org/10.1017/jfm.2019.616.

[13] Blake, W. K., "Mechanics of Flow-Induced Sound and Vibration, Volume 1 (Second Edition)," 2017. https://doi.org/https://doi.org/10.1016/B978-0-12-809273-6.00007-5, URL https://www.sciencedirect.com/science/article/pii/B9780128092736000075.